

## Three-state Potts model in combination with the rock-scissors-paper game

Attila Szolnoki and György Szabó

Research Institute for Technical Physics and Materials Science, P. O. Box 49, H-1525 Budapest, Hungary

Mária Ravasz

Department of Physics, Babeş-Bolyai University, RO-400084 Cluj, Romania

(Received 14 July 2004; published 14 February 2005)

We study a three-state Potts model extended by allowing cyclic dominance between the states as exemplified in the rock-scissors-paper game. Monte Carlo simulations are performed on a square lattice while varying the temperature and the strength of cyclic dominance. It is shown that the critical phase transition from the disordered state to the ordered one is destroyed by the cyclic dominance, which yields a self-organizing pattern even at low temperatures. The differences and similarities are discussed between the present model and half-filled, driven lattice gases with repulsive interaction.

DOI: 10.1103/PhysRevE.71.027102

PACS number(s): 05.50.+q, 05.10.Ln, 64.60.Cn

Ordering phenomena and related phase transitions are already well understood in equilibrium systems [1] while a theoretical understanding of nonequilibrium phase transitions is still in its infancy [2,3]. Many relevant and general features of these transitions in equilibrium systems can be studied by the Potts models [4]. We present an extended version of the three-state Potts model to investigate the effect of cyclic dominance between the states. We can imagine this model as a combination of the traditional Potts model and a spatial rock-scissors-paper game (sometimes known as three-state cyclic predator-prey or Lotka-Volterra models), this way providing a continuous transition between an equilibrium system and a spatial evolutionary game where the time-reversal symmetry (detailed balance) is broken at the elementary (microscopic) steps. The consideration of this model was strongly motivated by the work of Katz *et al.* [5,6] who presented the concept of driven lattice gases to study the effect of an external electric field on their ordering process. Since the appearance of their work, many general features of these systems have been explored (for a review see Refs. [2,7]).

In this Brief Report we will show that in the presence of cyclic dominance long-range order cannot be observed, and thereby the critical transition (observed in the traditional Potts model) is also suppressed. Instead, a self-organizing pattern is observed even for low temperatures and weak cyclic dominance. The behavior of the correlation length and specific heat also proves this fact. A similar phenomenon has already been observed for a two-dimensional driven lattice gas with repulsive interactions. There the formation of long-range order is prevented by an interfacial instability that results from the enhanced particle transport along the boundaries separating the “chessboard”- and “antichessboard”-ordered phases [8,9].

In our model the strength of cyclic dominance will be characterized by a single parameter ( $\varepsilon$ ) in such a way that for  $\varepsilon=0$ , the system becomes equivalent to the equilibrium Potts model: exhibiting a well-known critical transition. Our analysis is focused on a two-dimensional system where each site  $x$  of a square lattice is characterized by a three-state site variable, namely,  $s(x)=s_0, s_1$ , and  $s_2$ . For later convenience

these states (strategies, species, etc.) will be denoted by the basis vectors of a three-dimensional space, i.e.,

$$s_0 = \begin{pmatrix} 1 \\ 0 \\ 0 \end{pmatrix}, \quad s_1 = \begin{pmatrix} 0 \\ 1 \\ 0 \end{pmatrix}, \quad s_2 = \begin{pmatrix} 0 \\ 0 \\ 1 \end{pmatrix}. \quad (1)$$

The time evolution of the system is governed by random sequential updates. More precisely, the transition probability from a state  $s(x)$  (at site  $x$ ) to a randomly chosen state  $s'(x)$  is given as

$$W[s(x) \rightarrow s'(x)] = \frac{1}{1 + \exp[-\delta U(x)/T]}, \quad (2)$$

where  $\delta U(x)$  is the difference of payoffs between the final and initial states, and  $T$  is the temperature characterizing the effect of the noise. The payoff at site  $x$  depends on  $s(x)$  as well as on the neighboring states [ $s(y)$ ] as given by the following sum of matrix products:

$$U(x) = \sum_{\langle y \rangle} s^\dagger(x) A s(y), \quad (3)$$

where the summation runs over the nearest neighbors of the site  $x$ ,  $s^\dagger(x)$  denotes the transpose of  $s(x)$ , and the payoff matrix  $A$  is defined as

$$A = \begin{pmatrix} 1 & \varepsilon & -\varepsilon \\ -\varepsilon & 1 & \varepsilon \\ \varepsilon & -\varepsilon & 1 \end{pmatrix}. \quad (4)$$

In the limit  $\varepsilon \rightarrow 0$ , this model can be considered as a (kinetic) three-state ferromagnetic Potts model [4] with Glauber dynamics [10]. Plainly, in this case the total energy is defined as  $H = -\sum_x U(x)/2$  and the microscopic processes satisfy the detailed balance in equilibrium. Consequently, the system tends towards a stationary state whose statistical features are described by the Gibbs ensemble. When decreasing the temperature, the Potts model undergoes an ordering process from the disordered state to one of the three equivalent homogeneous (ordered) states. The corresponding criti-

cal transition represents a well-known universality class [1,4].

For  $\varepsilon > 0$  the off-diagonal components of the payoff matrix  $A$  are antisymmetric; therefore the total payoff (or the above-defined  $H$ ) is not affected by the value of  $\varepsilon$  for any state. At the same time, the value of  $\varepsilon$  influences the probability of strategy changes, because  $W[s(x) \rightarrow s'(x)]$  directly depends on the variations in individual payoffs  $[\delta U(x)]$ . The above evolutionary rule demonstrates a strategy in the (selfish) individuals attempt to maximize their own payoff without concerning themselves with their neighbors' performance. As a result, cyclic invasions occur along the boundaries separating homogeneous domains; domains of state  $s_0$  are invaded by  $s_1$ , which are invaded by  $s_2$ , which are invaded by  $s_0$ . These cyclic invasions are capable of maintaining a self-organizing pattern with rotating spiral arms whose "velocity" is controlled by  $\varepsilon$  [11–13].

For most of the spatial evolutionary games, the choice of the dynamical rules (or  $W[s(x) \rightarrow s'(x)]$ ) is based on a learning mechanism or strategy adoption modeling the Darwinian selections [14–16]. In these models different ways are suggested for the players to adopt the strategy of their more successful neighbors. A common feature of these strategy adoptions is that the new state will be equivalent to one of the neighboring strategies. Consequently, this mechanism prohibits the variation inside the homogeneous domains and makes the extinction process similar to those defined by the contact process (or directed percolation) [2,3]. In the present model, however, the above Glauber dynamics allow the players to choose all the possible strategies. Therefore, the time variation is not restricted to the interfaces separating the homogeneous domains. In the context of evolutionary game theory, the above evolutionary rule describes a different behavior. Namely, here the players know all the possibilities and their choices depend on the increase in income that they are able to predict, given their knowledge of neighboring strategies.

In the present work we study the effect of the "cyclic dominance" on the phase transition. For this purpose systematic Monte Carlo (MC) simulations are performed on a square lattice under periodic boundary conditions varying the temperature  $T$  and strength  $\varepsilon$  of the cyclic dominance for different linear sizes  $L$ . Each simulation is started from a random initial state and after a suitable thermalization time, we recorded the concentration of states ( $\rho_0$ ,  $\rho_1$ , and  $\rho_2$ ) for each Monte Carlo step. We have also made simulations starting from ordered homogeneous phases to check the stability of the stationary state. To investigate the ordering process, we have determined the average value of the order parameter from the values of concentration data [4,17]

$$m = \frac{1}{2} \langle [3 \max(\rho_0, \rho_1, \rho_2) - 1] \rangle, \quad (5)$$

where  $\langle \dots \rangle$  refers to averaging over a sampling time varied from  $10^5$  to  $10^6$  Monte Carlo steps per sites (MCS). In the disordered phases  $\rho_0 = \rho_1 = \rho_2 = 1/3$  (due to the cyclic symmetry) and  $m=0$  in the thermodynamic limit ( $L \rightarrow \infty$ ). For  $\varepsilon=0$  and below the critical temperature [ $T < T_c = 0.995(1)$ ]

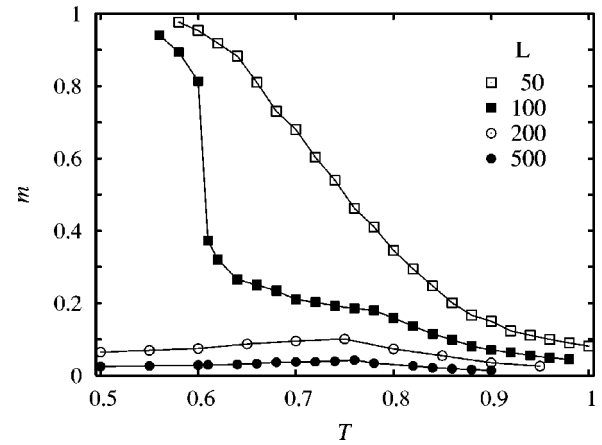


FIG. 1. Monte Carlo data for the order parameter vs. temperature at  $\varepsilon=0.1$  for different system sizes as indicated. The solid lines are visual guides.

the system evolves into one of the long-range ordered (symmetry-breaking) stationary states [e.g.,  $\langle \rho_0 \rangle = (1+2m)/3$  and  $\langle \rho_1 \rangle = \langle \rho_2 \rangle = (1-m)/3$  and the remaining two equivalent states are given by the cyclic permutation of indices] if the linear size is sufficiently large. In the thermodynamic limit the order parameter  $m$  decreases monotonously from 1 to 0 as the temperature is increased from 0 to  $T_c$  and the vanishing of  $m$  follows a power law behavior if  $T_c$  is approached from below [4]. For finite sizes, however, the MC simulations exhibit a smoothed-order parameter function that deviates monotonously if we decrease the system size [17,18]. Significantly, different finite size effects are observed when investigating the present model for  $\varepsilon > 0$ .

Figure 1 illustrates how the order parameter  $m$  varies with temperature  $T$  for different linear sizes if  $\varepsilon=0.1$ . MC data referring to an ordering process for small sizes ( $L=50$  and  $100$ ) bear a resemblance to MC data obtained for  $\varepsilon=0$ . On the contrary, for example when  $L=500$ , the MC data do not indicate the appearance of long-range order. Instead, a self-organizing, three-color domain structure can be observed when visualizing the time-dependence of the spatial distribution (for a snapshot, see Fig. 2).

On this snapshot one can identify all three ordered phases forming domains with a characteristic linear size  $l$ . For  $T < T_c$  and  $\varepsilon=0$ , the growth of these domains ( $l \sim \sqrt{t}$ ) is driven by the interfacial (Potts) energy [19–21]. Here, however, this domain growth is prevented by two processes emerging for  $\varepsilon > 0$ . The first process is related to the appearance of rotating spiral arms for the three-edge vortices where the three types of domains (or domain boundaries) meet. On these maps we can distinguish vortices and antivortices rotating in opposite directions. Some topological and geometrical features of such spatiotemporal patterns were already investigated in previous papers [11–13,22]. It is found that the spirals become well marked if a "surface tension" is switched on, after which the corresponding patterns cannot be characterized by a single parameter (e.g., typical domain size or correlation length) [22].

In the present model there exists a second process causing the appearance of growing domains via a nucleation mecha-

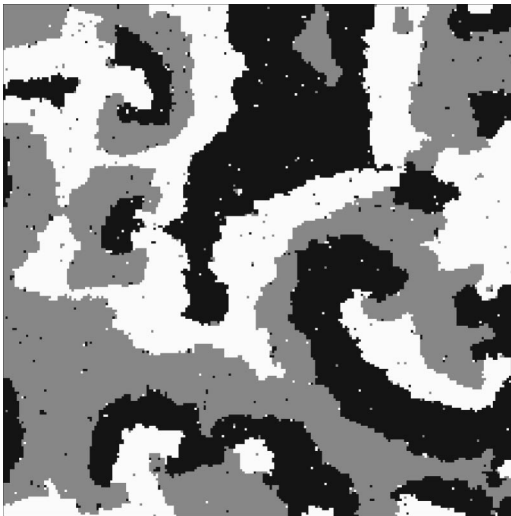


FIG. 2. Snapshot of a typical domain structure appearing for  $T = 0.64$  and  $\varepsilon = 0.1$ . The three-edge vortices (antivortices) rotate in a clockwise (anticlockwise) direction with spiral arms because the average velocity of the invasion fronts (white invades black invades gray invades white) is hardly affected by their curvature.

nism inside the large “homogeneous” territories. Due to this process, an “ordered state” dominated by  $s_0$  will be transformed into another one dominated by  $s_1$  as indicated by simulations for small sizes. In these cases the three ordered states follow each other cyclically and the above method yields a sufficiently large value for  $m$  (see Fig. 1). Both the duration time and the probability of these transitions—which are initiated by a nucleation mechanism dependent upon the thermal fluctuations—increase with the system size. This is the reason why the values of  $m$  are higher for  $L = 50$  than those for  $L = 100$  in Fig. 1.

For sufficiently large system sizes ( $L \gg l$ ), both mentioned mechanisms work simultaneously and result in a self-organizing pattern where the three states are present with the same concentration and  $m = 0$ . Henceforth, the quantitative investigations will be focused on large systems ( $L > 500$ ) and the temperature region ( $T > 0.6T_c$ ) where the spatial patterns are isotropic.

We now turn our focus to the variation of the correlation length  $\xi$ , derived from the asymptotic behavior (exponential vanishing) of the two-site correlation function [8]. For this purpose a series of MC simulations were performed by varying the temperature for  $\varepsilon = 0.1$ . The inset in Fig. 3 illustrates the absence of divergence in  $\xi$  as expected. When decreasing the temperature, the correlation length increases monotonously until a maximum value [ $\xi \approx 11.5(5)$  measured in lattice unit]. Below the peak at  $T \approx 0.77$  the visualization of the distribution of species shows a self-organizing pattern (see Fig. 2) and here the value of  $\xi$  decreases very slowly with  $T$ .

The  $\varepsilon$  dependence of the correlation length is also determined for a fixed temperature and the results are illustrated in a log-log plot (see Fig. 3). These MC data are consistent with a predicted  $\xi \sim 1/\varepsilon$  for small  $\varepsilon$ . For a typical domain size a similar divergence was found previously in a model where the nucleation mechanism was blocked [22]. This

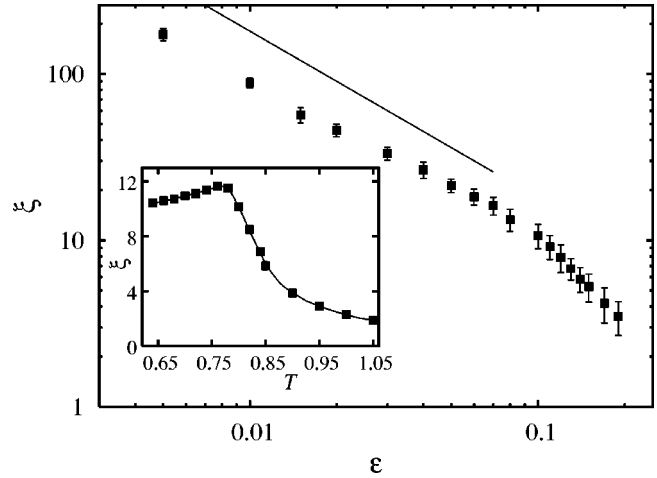


FIG. 3. Variation of correlation length (with error bars) as a function of  $\varepsilon$  for fixed temperature ( $T = 0.75$ ). The straight line indicates a power law divergence with a slope of  $-1$ . The inset shows the correlation length vs temperature for  $\varepsilon = 0.1$ .

observation refers to the minor role that the nucleation plays in the maintenance of self-organizing patterns at sufficiently low temperature ( $T < T_c$ ). For higher temperature, the nucleation mechanism plays a crucial role by preventing the formation of a monodomain state even for  $\varepsilon = 0$ . Thus it is conjectured that this process results in a different behavior of  $\xi$  at the critical temperature. Furthermore, it is worth mentioning here that in the above-mentioned driven lattice gas model, the transversal correlation length was also proportional to the inverse of the strength of driving field [9].

In our model the Potts energy measures the concentration of domain walls and also gives additional information about spatial distributions. From the average Potts energy as a function of temperature, one can derive a specific heat ( $c = d\langle H \rangle / dT$ ) that exhibits a  $\lambda$  divergence at the critical temperature in the equilibrium limit ( $\varepsilon = 0$ ). Figure 4 illustrates how the  $\lambda$  divergence is smoothed out if the cyclic domi-

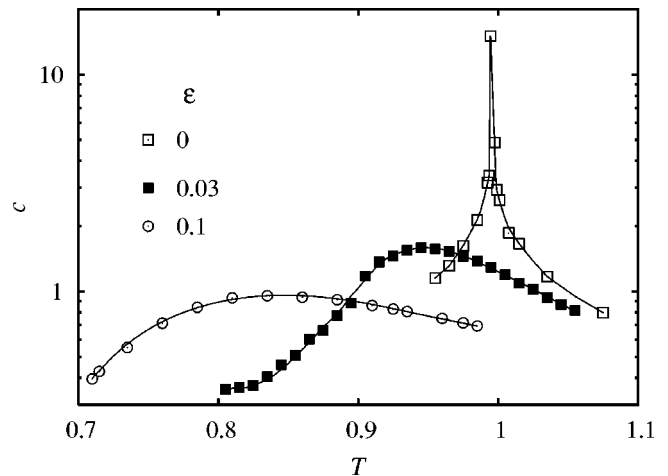


FIG. 4. Specific heat as a function of temperature for three different values of  $\varepsilon$  as indicated. These MC data are obtained for such a large linear size ( $L = 1000$ ) that size effects are negligible.

nance is switched on. When choosing larger and larger  $\varepsilon$  the maximum value of specific heat decreases, while the peak position moves towards lower and lower temperatures. The peaks are so shallow in the “driven” cases that a logarithmic scale was necessary to present them in the same figure. The appearance of this peak in the specific heat can be interpreted as a sign of short-range ordering.

A similar phenomenon was observed for the driven lattice gases with repulsive interaction when increasing the external electric field [8,9]. Although the observed patterns and microscopic mechanisms are very different, in both cases interfacial effects prevent the formation of long-range order in the presence of the driving force. In these cases the interfaces belong to the stationary states and their geometrical characterization requires additional parameters. This general feature can occur in other nonequilibrium systems (e.g., in ecological models) where an external force induces some extra activity along the interfaces separating the “ordered domains.”

In summary, a three-state dynamical lattice model was introduced by combining the Potts model and the rock-scissors-paper game to study the effect of cyclic dominance on ordering processes. The cyclic dominance was shown to break the time-reversal symmetry at the elementary steps, whereby the behavior of this model cannot be described by methods of equilibrium statistical physics. Our numerical analyses have demonstrated that both the long-range (symmetry-breaking) ordering process and the corresponding critical transition are suppressed in the presence of cyclic dominance ( $\varepsilon > 0$ ). As seen in the simulations, the three equivalent ordered phases coexist by forming a self-organizing domain structure even at low temperatures and weak cyclic dominance. The equilibrium state is approached via the divergence of the typical domain size when the strength of cyclic dominance goes to zero.

This work was supported by the Hungarian National Research Fund under Grant No. T-47003.

- 
- [1] H. E. Stanley, *Introduction to Phase Transitions and Critical Phenomena* (Clarendon Press, Oxford, 1971).
- [2] J. Marro and R. Dickman, *Nonequilibrium Phase Transitions in Lattice Models* (Cambridge University Press, Cambridge, 1999).
- [3] H. Hinrichsen, *Adv. Phys.* **49**, 815 (2000).
- [4] F. Y. Wu, *Rev. Mod. Phys.* **54**, 235 (1982).
- [5] S. Katz, J. L. Lebowitz, and H. Spohn, *Phys. Rev. B* **28**, 1655 (1983).
- [6] S. Katz, J. L. Lebowitz, and H. Spohn, *J. Stat. Phys.* **34**, 497 (1984).
- [7] B. Schmittmann and R. K. P. Zia, *Statistical Mechanics of Driven Diffusive Systems* (Academic Press, Oxford, 1995).
- [8] G. Szabó, A. Szolnoki, and T. Antal, *Phys. Rev. E* **49**, 299 (1994).
- [9] G. Szabó, A. Szolnoki, T. Antal, and I. Borsos, *Phys. Rev. E* **55**, 5275 (1997).
- [10] R. J. Glauber, *J. Math. Phys.* **4**, 294 (1963).
- [11] K. I. Tainaka, *Phys. Rev. E* **50**, 3401 (1994).
- [12] L. Frachebourg, P. L. Krapivsky, and E. Ben-Naim, *Phys. Rev. E* **54**, 6186 (1996).
- [13] G. Szabó, M. A. Santos, and J. F. F. Mendes, *Phys. Rev. E* **60**, 3776 (1999).
- [14] M. A. Nowak and R. M. May, *Int. J. Bifurcation Chaos Appl. Sci. Eng.* **3**, 35 (1993).
- [15] C. Hauert, *Int. J. Bifurcation Chaos Appl. Sci. Eng.* **12**, 1531 (2002).
- [16] G. Szabó and C. Toke, *Phys. Rev. E* **58**, 69 (1998).
- [17] M. S. S. Challa, D. P. Landau, and K. Binder, *Phys. Rev. B* **34**, 1841 (1986).
- [18] D. P. Landau and K. Binder, *A Guide to Monte Carlo Simulations in Statistical Physics* (Cambridge University Press, Cambridge, 2000).
- [19] A. J. Bray, *Adv. Phys.* **43**, 357 (1994).
- [20] G. S. Grest, M. P. Anderson, and D. J. Srolovitz, *Phys. Rev. B* **38**, 4752 (1988).
- [21] O. G. Mouritsen, *Int. J. Mod. Phys. B* **4**, 1925 (1990).
- [22] G. Szabó and A. Szolnoki, *Phys. Rev. E* **65**, 036115 (2002).